**Coupled Systems Mechanics,** *Vol. 11, No. 6 (2022) 543-556*
https://doi.org/10.12989/csm.2022.11.6.543 

# Delamination analysis of multilayered beams with non-linear stress relaxation behavior

Victor I. Rizov*

*Department of Technical Mechanics, University of Architecture, Civil Engineering and Geodesy, 1 Chr. Smirnensky Blvd., 1046-Sofia, Bulgaria*

*(Received July 18, 2022, Revised September 6, 2022, Accepted September 7, 2022)*

**Abstract.** Delamination of multilayered inhomogeneous beam that exhibits non-linear relaxation behavior is analyzed in the present paper. The layers are inhomogeneous in the thickness direction. The dealamination crack is located symmetrically with respect to the mid-span. The relaxation is treated by applying a non-linear stress-strain-time constitutive relation. The material properties which are involved in the constitutive relation are distributed continuously along the thickness direction of the layer. The delamination is analyzed by applying the *J*-integral approach. A time-dependent solution to the *J*-integral that accounts for the non-linear relaxation behavior is derived. The delamination is studied also in terms of the time-dependent strain energy release rate. The balance of the energy is analyzed in order to obtain a non-linear time-dependent solution to the strain energy release rate. The fact that the strain energy release rate is identical with the *J*-integral value proves the correctness of the non-linear solutions derived in the present paper. The variation of the *J*-integral value with time due to the non-linear relaxation behavior is evaluated by applying the solution derived.

**Keywords:** delamination; inhomogeneous material; multilayered structure; non-linear relaxation; time-dependent behavior

## 1. Introduction

The advance in various areas of current engineering is closely related to the application of high performance structural materials. In particular, the multilayered materials and structures are of great interest. Another exceptionally perspective class of structural materials are the inhomogeneous (functionally graded) materials (Ali Kurşun *et al.* 2012, Ali Kurşun and Muzaffer Topçu 2013, Ali Kurşun *et al.* 2014, Arefi and Rahimi 2013, Arefi 2014, 2015, Butcher *et al.* 1999, Dolgov 2002, Gasik 2010, Han *et al.* 2001, Hedia *et al.* 2014, Hirai and Chen 1999, Mahamood and Akinlabi 2017). Such materials are widely used in modern technology since they have numerous advantages over the homogeneous structural materials (Markworth *et al.* 1995, Miyamoto *et al.* 1999, Nemat-Allal *et al.* 2011, Saiyathibrahim *et al.* 2016, Shrikantha and Gangadharan 2014, Nguyen *et al.* 2015, Nguyen *et al.* 2020, Wu *et al.* 2014). Particularly, high strength-to-weight and stiffness-to-weight ratios is the most advantageous feature of layered

*Corresponding author, Professor, E-mail: V_RIZOV_FHE@UACG.BG

 ISSN: 2234-2184 (Print), 2234-2192 (Online)

materials especially for load-bearing structural applications in which the low weight is of primary concern.

However, along with their advantages, the multilayered materials have some fundamental drawbacks. For example, the use of multilayered materials and structures is hindered because of their low delamination resistance. Appearance of delamination cracks between layers is one of the main reasons for failure of multilayered structural members. Therefore, analyzing the delamination fracture of multilayered beam structures is a research problem of great importance in the context of ensuring of structural integrity, safety and durability. The delamination has been analyzed usually assuming linear-elastic behavior (Dolgov 2005, 2016). Recently, papers concerned with delamination analyses of multilayered inhomogeneous non-linear elastic beam configurations have also been published (Rizov 2019, 2020, Rizov and Altenbach 2020, 2022, 2022a, Rizov 2022). Analyses of delamination in inhomogeneous beams under linear relaxation have been developed too (Rizov 2020a).

In contrast to (Rizov 2020a), the main goal of the present paper is to analyze the delamination of a multilayered inhomogeneous beam structure that exhibits non-linear relaxation behavior. The significance of the present research work consists in the fact that in the engineering practice the delamination and the non-linear relaxation behaviour can be combined since there are load-bearing multilayered structural applications in which the engineering structures are under constant strains (the strains do not change with time). In such situations, the structures may exhibit non-linear relaxation behaviour that should be taken into account when analyzing the delamination of these multilayered structures (this is done in the present paper).

A time-dependent solution to the *J*-integral that takes into account the non-linear relaxation is derived here. A time-dependent solution to the strain energy release rate is also derived in order to verify the *J*-integral solution. The variation of the *J*-integral with the time is investigated.

## 2. Delaminated multilayered beam under non-linear relaxation

The multilayered inhomogeneous beam configuration shown in Fig. 1 is under consideration in the present paper. The beam is made of adhesively bonded layers of individual thicknesses and material properties. The number of layers is arbitrary. In order to create conditions for delamination fracture, a notch of depth, $h_2$, is cut-out in the beam as shown in Fig. 1. A delamination crack of length, $2a$, is located between layers. The thicknesses of the lower and upper delamination crack arms are denoted by $h_1$ and $h_2$, respectively. The length of the beam is $l$. The beam has a rectangular cross-section of width, $b$, and thickness, $h$. The beam is loaded at its two ends by bending moments and then held so as the angle of rotation, $\phi$, of the ends of the beam does not change with time (Fig. 1). The stresses in the layers of the beam decrease with the time while the strains remain constant, i.e., the layers of the beam exhibit relaxation behavior that is treated by using the following non-linear stress-strain-time constitutive relation (Dowling 2013)

$$\sigma_i = \frac{H_i \varepsilon}{\left[1 + tD_i H_i^{n_i} (n_i - 1) \varepsilon^{n_i - 1}\right]^{\frac{1}{n_i - 1}}}, \tag{1}$$

where

$$i = 1, 2, ..., m_2. \tag{2}$$

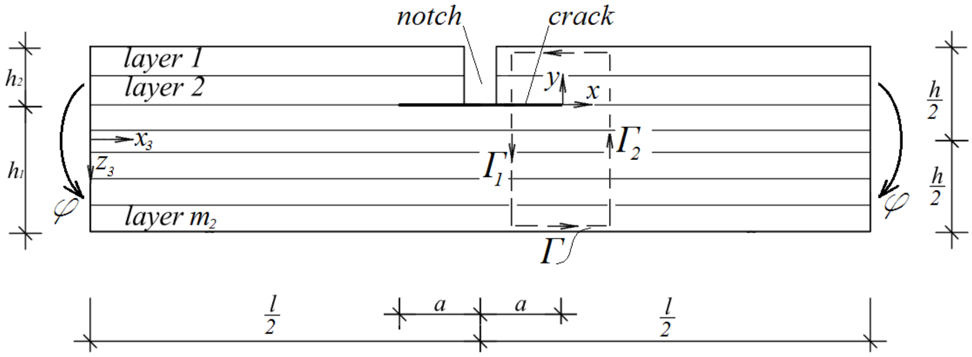


Fig. 1 Multilayered inhomogeneous beam with a delamination crack

In the above formulae, $\varepsilon$ is the strain, $t$ is time, $\sigma_i$ is the stress in the $i$-th layer of the beam, $H_i$, $D_i$ and $n_i$ are material properties in the layer, $m_2$ is the number of layers in the beam. The material property, $H_i$, corresponds to the modulus of elasticity (since only elastic strain occurs as a result of rapid initial loading, at $t = 0$ formula (1) transforms in $\sigma_i = H_i\varepsilon$; therefore, $H_i$ corresponds to the modulus of elasticity in the $i$-th layer of the beam). The material property, $D_i$, accounts for relaxation behaviour. At $D_i = 0$ the material exhibits linear-elastic behaviour. In the case of linear relaxation, the parameter, $D_i$, is related to the coefficient of viscosity, $\eta_i$, by the formula $\eta_i = 1/D_i$ (Dowling 2013). The material property, $n_i$, accounts for nonlinearity in the $i$-th layer of the beam. The units for $H_i$ and $D_i$ are Pa and 1/(Pa.s), respectively. $n_i$ is dimensionless quantity.

The material in each layer is inhomogeneous along the thickness (therefore, the material properties vary continuously along the thickness of the layer (refer to formulae (3)-(5)).

The distributions of $H_i$, $D_i$ and $n_i$ along the thickness of the $i$-th layer are written as

$$H_i = \frac{H_{B_i}}{1 + f_i \dfrac{z_1 - z_{1i}}{z_{1i+1} - z_{1i}}}, \tag{3}$$

$$D_i = \frac{D_{B_i}}{1 + g_i \dfrac{z_1 - z_{1i}}{z_{1i+1} - z_{1i}}}, \tag{4}$$

$$n_i = \frac{n_{B_i}}{1 + s_i \dfrac{z_1 - z_{1i}}{z_{1i+1} - z_{1i}}}, \tag{5}$$

where

$$z_{1i} \le z_1 \le z_{1i+1}. \tag{6}$$

In formulae (3)-(6), $H_{B_i}$, $D_{B_i}$ and $n_{B_i}$ are the values of $H_i$, $D_i$ and $n_i$ in the upper surface of the $i$-th layer, $f_i$, $g_i$ and $s_i$ are material parameters which control the distributions of $H_i$, $D_i$ and $n_i$ in the thickness direction of the layer, $z_{1i}$ and $z_{1i+1}$ are the coordinates of the upper and lower surfaces of the layer, respectively (Fig. 2).

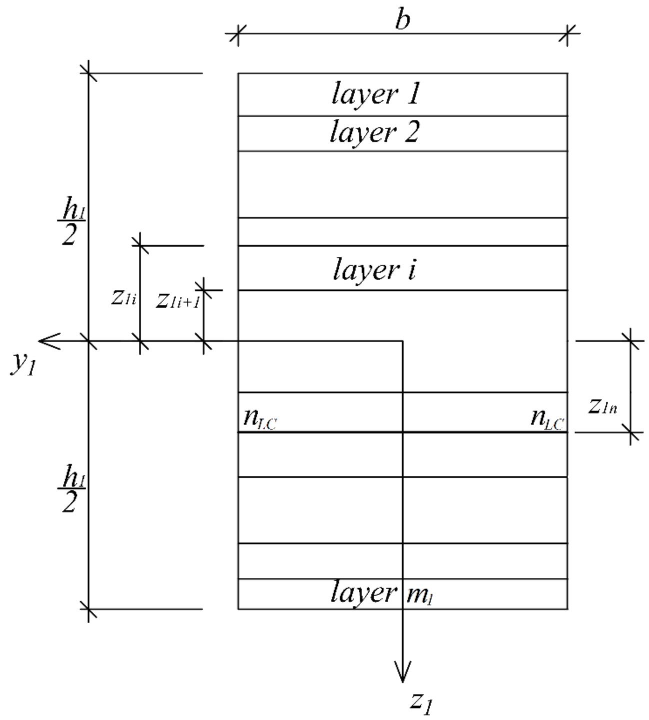


Fig. 2 Cross-section of the lower crack arm

Since the beam is symmetric with respect to $x_3 = l/2$, only half of the beam, $l/2 \leq x_3 \leq l$, is considered (Fig. 1).

Due to the relaxation, the multilayered inhomogeneous beam configuration exhibits time-dependent delamination behavior that is analyzed by applying the *J*-integral approach (Broek 1986).

Time-dependent solution to the *J*-integral is obtained by using the integration contour, Γ, shown by dashed line in Fig. 1. The upper delamination crack arm is free of stresses. Therefore, the solution to the *J*-integral is found as

$$J = 2(J_{\Gamma_1} + J_{\Gamma_2}), \tag{7}$$

where $J_{\Gamma_1}$ and $J_{\Gamma_2}$ are the values of the *J*-integral in segments, $\Gamma_1$ and $\Gamma_2$, of the integration contour.

The material in each layer is inhomogeneous along the thickness.

The segments, $\Gamma_1$ and $\Gamma_2$, coincide with the cross-sections of the lower crack arm and the un-cracked beam portion, respectively. It should be mentioned that the right-hand side of (7) is doubled in view of the symmetry (Fig. 1).

The *J*-integral is segment, $\Gamma_1$, of the integration contour is written as

$$J_{\Gamma_1}(t) = \sum_{i=1}^{i=m_1} \int_{z_{1i}}^{z_{1i+1}} \left[ u_{01i} \cos\alpha - \left( p_{xi} \frac{\partial u}{\partial x} + p_{yi} \frac{\partial v}{\partial x} \right) \right] ds \tag{8}$$

where $m_1$ is the number of layers in the lower crack arm, $u_{01i}$ is the strain energy density in the *i*-

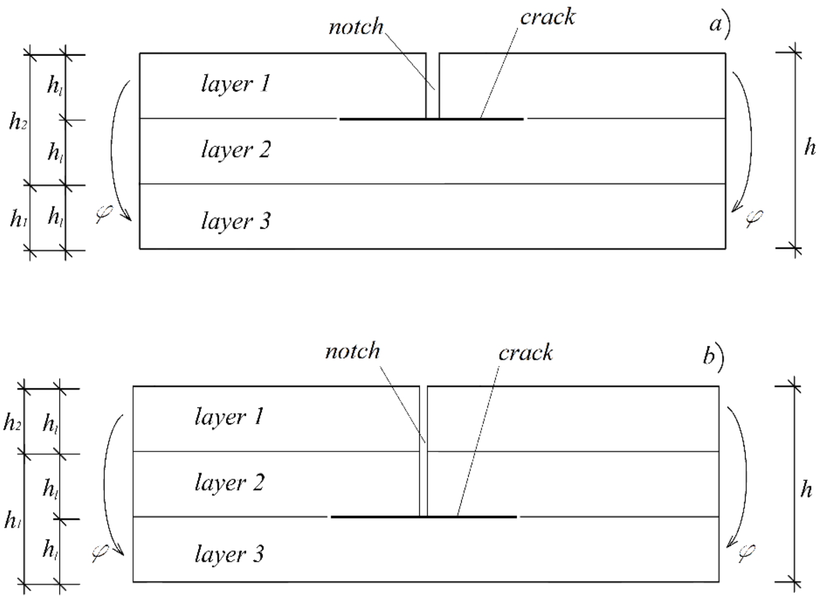


Fig. 3 Three-layered beam configurations with a delamination crack located (a) between layers 1 and 2, and (b) between layers 2 and 3

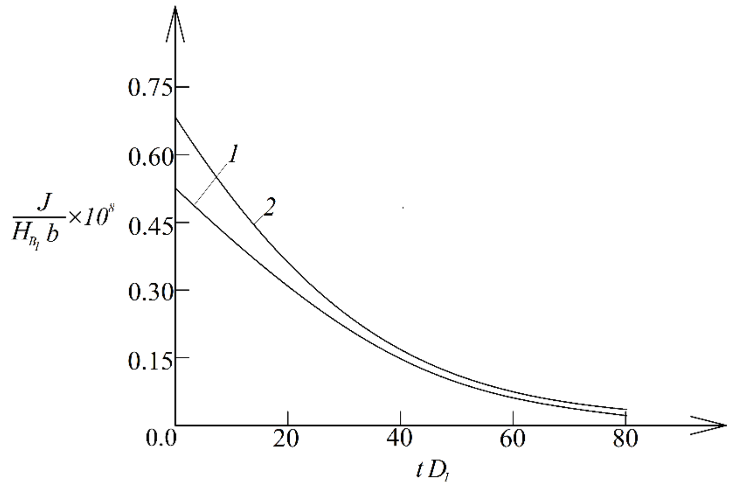


Fig. 4 The $J$-integral value in non-dimensional form presented as a function of the non-dimensional time (curve 1-for delamination crack located between layers 1 and 2, and curve 2-for delamination crack located between layers 2 and 3)

th layer, $\alpha$ is the angle between the outwards normal vector to the contour of integration and the crack direction, $p_{xi}$ and $p_{yi}$ are the stress vector components in the layer, $u$ and $v$ are the components of displacement vector with respect to the crack tip coordinate system $xy$, $ds$ is a differential element along the integration contour.

The strain energy density is equal numerically to the area enclosed by the stress-strain curve. Therefore, the strain energy density in the $i$-th layer is expressed as

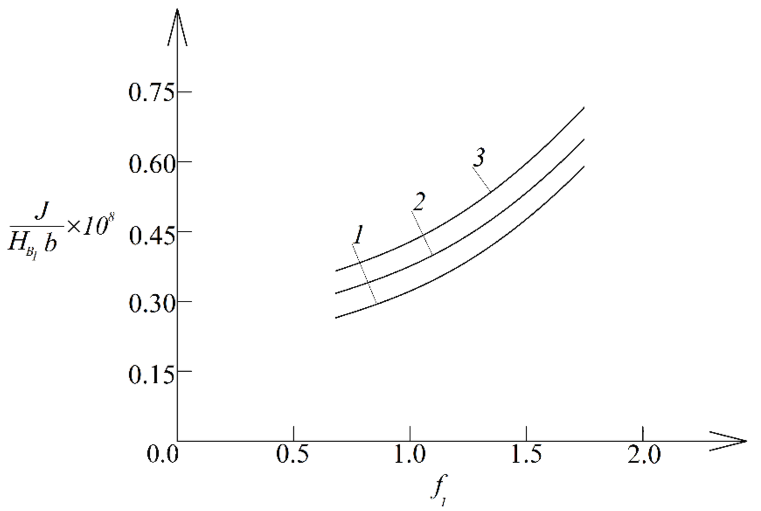


Fig. 5 The *J*-integral value in non-dimensional form presented as a function of $f_1$ (curve 1 - at $\phi = 0.002$ rad, curve 2 - at $\phi = 0.003$ rad and curve 3 - at $\phi = 0.004$ rad) (case b) from Fig. 3 is considered)

$$u_{01i}(z_1, t) = \int_0^{\varepsilon} \sigma_i d\varepsilon . \tag{9}$$

The other quantities which are involved in (8) are found as

$$p_{xi} = -\sigma_i \ , \tag{10}$$

$$p_{yi} = 0 \, , \tag{11}$$

$$ds = dz_1 \, , \tag{12}$$

$$\cos\alpha = -1 \, , \tag{13}$$

$$\frac{\partial u}{\partial x} = \varepsilon \ . \tag{14}$$

In the present paper, a beam of high length-to-thickness ratio is under consideration. Therefore, the distribution of the strains is treated by applying the Bernolli's hypothesis for plane sections.

Hence, the strain is distributed linearly along the thickness of the lower delamination crack arm

$$\varepsilon = \kappa_1 (z_1 - z_{1n}) \, , \tag{15}$$

where

$$-\frac{h_1}{2} \leq z_1 \leq \frac{h_1}{2} . \tag{16}$$

In formula (15), $\kappa_1$ is the curvature of the lower crack arm, $z_{1n}$ is the coordinate of the neutral axis (the position of the neutral axis is marked by $n_{LC} - n_{LC}$ in Fig. 2). The curvature and the

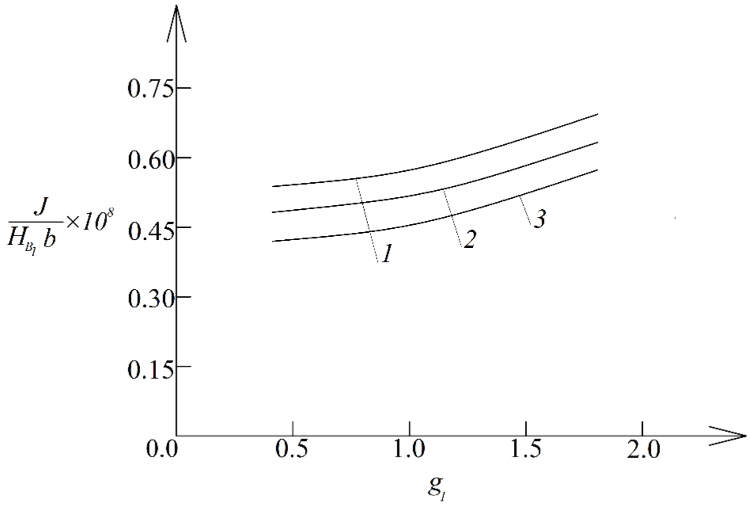


Fig. 6 The $J$-integral value in non-dimensional form presented as a function of $g_1$ (curve 1 - at $h_l = 0.002$ m, curve 2-at $h_l = 0.0025$ m and curve 3-at $h_l = 0.003$ m) (case b) from Fig. 3 is considered)

coordinate of the neutral axis are determined in the following way. First, three equations are worked-out by using the following conditions for equilibrium of the lower delamination crack arm and the un-cracked portion of the beam:

$$N_1 = 0, \tag{17}$$

$$N_2 = 0, \tag{18}$$

$$M_1 = M_2, \tag{19}$$

where $N_1$ and $N_2$ are the axial forces in the lower crack arm and the un-cracked beam portion, $M_1$ and $M_2$ are the bending moments in the lower crack arm and the un-cracked beam portion, respectively. The axial forces and bending moments in (17), (18) and (19) are expressed through the stresses.

Hence, Eqs. (17), (18) and (19) take the form

$$\sum_{i=1}^{i=m_1} \int_{z_{1i}}^{z_{1i+1}} \sigma_i dz_1 = 0, \tag{20}$$

$$\sum_{i=1}^{i=m_2} \int_{z_{2i}}^{z_{2i+1}} \sigma_{iUN} z_2 dz_2 = 0, \tag{21}$$

$$\sum_{i=1}^{i=m_1} \int_{z_{1i}}^{z_{1i+1}} \sigma_i z_1 dz_1 = \sum_{i=1}^{i=m_2} \int_{z_{2i}}^{z_{2i+1}} \sigma_{iUN} z_2 dz_2, \tag{22}$$

where $z_{2i}$ and $z_{2i+1}$ are the coordinates of the upper and lower surfaces of the $i$-th layer in the un-cracked portion of the beam, $z_2$ is the vertical centroidal axis of the cross-section of the un-cracked beam portion, $m_2$ is the number of layers in the beam, $\sigma_{iUN}$ is the stress in the $i$-th layer of the un-

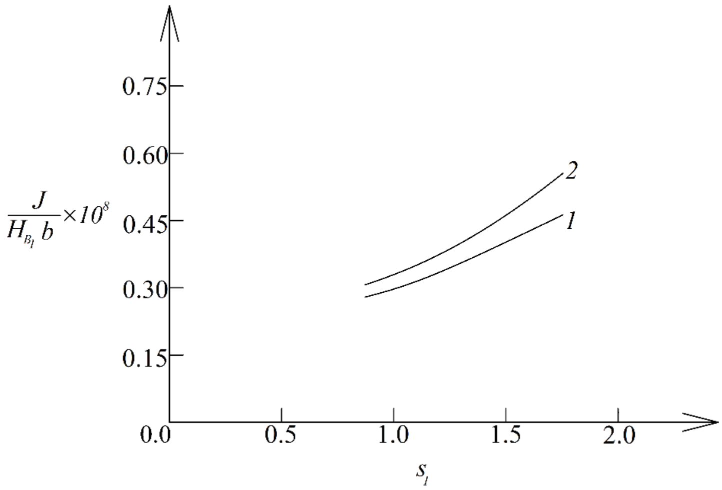


Fig. 7 The *J*-integral value in non-dimensional form presented as a function of $s_1$ (curve 1-for the beam with delamination between layers 1 and 2, curve 2-for the beam with delamination between layers 2 and 3)

cracked beam portion. $\sigma_{iUN}$ is found by replacing of $\varepsilon$ with $\varepsilon_{UN}$ in (1). Here, $\varepsilon_{UN}$ is the strain in the un-cracked beam portion.

Formula (15) is applied to obtain $\varepsilon_{UN}$. For this purpose, $\kappa_1$, $z_{1n}$ and $z_1$ are replaced with $\kappa_2$, $z_{2n}$ and $z_2$, respectively. Here, $\kappa_2$ and $z_{2n}$ are the curvature and the coordinate of the neutral axis of the un-cracked beam portion, respectively.

Further one equation is worked-out by expressing the angle of rotation, $\phi$, as a function of $\kappa_1$ and $\kappa_2$. For this purpose, the integrals of Maxwell-Mohr are applied. The result is

$$\varphi = \kappa_1 a + \kappa_2 \left( \frac{l}{2} - a \right). \tag{23}$$

After substituting of stresses in (20), (21) and (22), the three equations for equilibrium are solved with equation (23) with respect to $\kappa_1$ , $z_{1n}$, $\kappa_2$ and $z_{2n}$ by using the MatLab computer program.

The *J*-integral in segment, $\Gamma_2$, is written as

$$J_{\Gamma_2}(t) = \sum_{i=1}^{i=m_2} \int_{z_{2i}}^{z_{2i+1}} \left[ u_{02i} \cos\alpha_2 - \left( p_{xi_2} \frac{\partial u}{\partial x_2} + p_{yi_2} \frac{\partial v}{\partial x_2} \right) \right] ds_2 \ , \tag{24}$$

where

$$p_{xi_2} = \sigma_{iUN} \ , \tag{25}$$

$$p_{yi_2} = 0 , \tag{26}$$

$$ds_2 = -dz_2 , \tag{27}$$

$$\cos\alpha_2 = 1 , \tag{28}$$

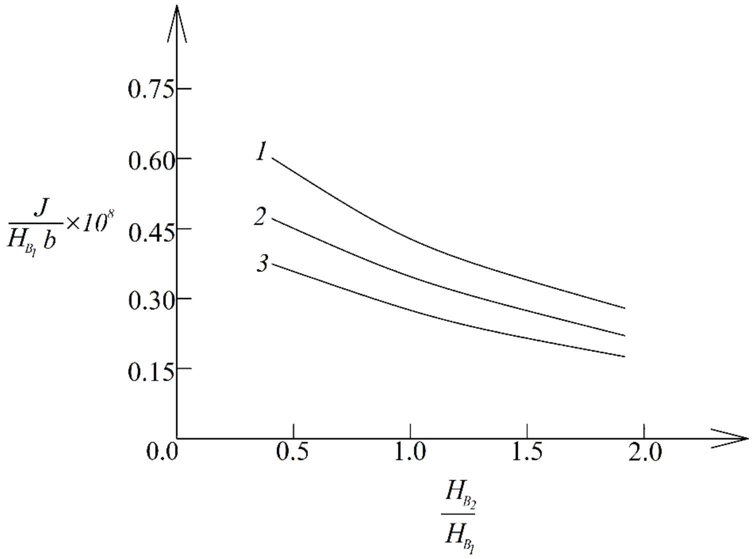


Fig. 8 The *J*-integral value in non-dimensional form presented as a function of $H_{B_2}/H_{B_1}$ ratio (curve 1-at $H_{B_3}/H_{B_1} = 0.5$, curve 2-at $H_{B_3}/H_{B_1} = 1.5$ and curve 3-at $H_{B_3}/H_{B_1} = 2.5$)

$$\frac{\partial u}{\partial x_2} = \varepsilon_{UN} \ . \tag{29}$$

The *J*-integral solution is found by substituting of (8) and (24) in (7). The integration is carried-out by using the MatLab computer program. It should be mentioned that this solution to the *J*-integral is time-dependent. Therefore, the solution can be applied to evaluate the non-linear relaxation induced variation of the *J*-integral value with the time.

The delamination in the multilayered inhomogeneous beam is analyzed also in terms of the strain energy release rate, $G$. For this purpose, a time-dependent solution to the strain energy release rate is derived by considering the balance of the energy in the beam. A small increase, $\Delta a$, of the delamination crack length is assumed. The balance of the energy is written as

$$M\delta\varphi = \frac{\Delta U}{\Delta a}\delta a + Gb\delta a \ . \tag{30}$$

where $U$ is the strain energy cumulated in the beam. From (3), one derives

$$G(t) = 2\left(\frac{M}{b}\frac{\partial \varphi}{\partial a} - \frac{1}{b}\frac{\partial U}{\partial a}\right). \tag{31}$$

It should be noted that the term in brackets in (31) is doubled in view of the symmetry (Fig. 1).

The strain energy is written as

$$U(a,t) = ab\sum_{i=1}^{i=m_1}\int_{z_{1i}}^{z_{1i+1}} u_{01i}dz_1 + \left(\frac{l}{2} - a\right)b\sum_{i=1}^{i=m_2}\int_{z_{2i}}^{z_{2i+1}} u_{02i}dz_2 \ . \tag{32}$$

By substituting of (23) and (32) in (31), one obtains

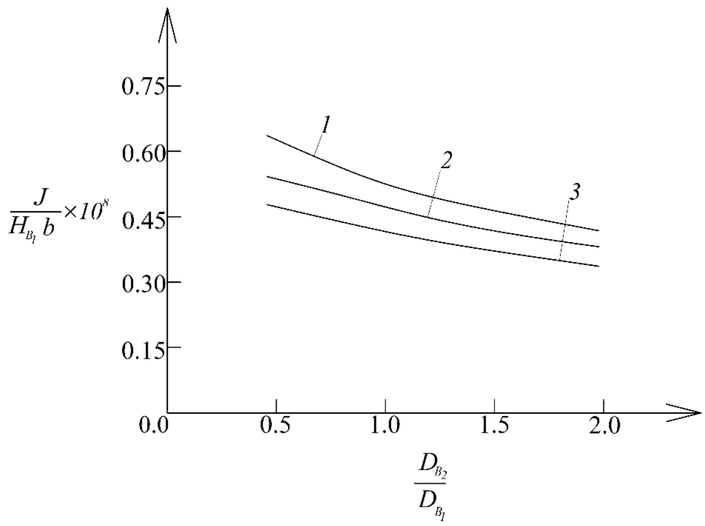


Fig. 9 The *J*-integral value in non-dimensional form presented as a function of $D_{B_2}/D_{B_1}$ ratio (curve 1-at $D_{B_3}/D_{B_1} = 0.5$, curve 2-at $D_{B_3}/D_{B_1} = 1.5$ and curve 3-at $D_{B_3}/D_{B_1} = 2.5$)

$$G(t) = 2\left[ \frac{M}{b}(\kappa_1 - \kappa_2) - \left( \sum_{i=1}^{i=m_1} \int_{z_{1i}}^{z_{1i+1}} u_{01i} dz_1 - \sum_{i=1}^{i=m_2} \int_{z_{2i}}^{z_{2i+1}} u_{02i} dz_2 \right) \right]. \tag{33}$$

The MatLab computer program is applied to perform the integration in (33). The fact that the strain energy release rate found by (33) matches exactly the *J*-integral value obtained by (7) proves the correctness of delamination analysis of multilayered inhomogeneous beam with non-linear relaxation behavior developed in the present paper.

## 3. Numerical results

In this section of the paper, numerical results are presented by using the time-dependent solution to the *J*-integral obtained in section 2. The *J*-integral is expressed in non-dimensional form by applying the formula $J_N = J/(H_{B_1} b)$. Two three-layered beam configurations are analyzed in order to evaluate the effect of delamination crack location along the beam thickness on the *J*-integral value (Fig. 3). A delamination crack is located between layers 2 and 3 in the three-layered beam depicted in Fig. 3(b). A three-layered beam with a delamination crack between layers 1 and 2 is also considered (Fig. 3(a)). The thickness of each layer in the two three-layered beam configurations in Fig. 3 is $h_l$. It is assumed that $h_l = 0.002$ m, $h = 0.006$ m, $b = 0.005$ m and $\phi = 0.004$ rad.

The variation of the *J*-integral value with the time is investigated for both three-layered beam configurations depicted in Fig. 3. For this purpose, calculations of the *J*-integral values are carried-out at various values of the time. The results obtained are illustrated in Fig. 4 where the *J*-integral value in non-dimensional form is presented as function of the non-dimensional time for the two three-layered beams (the time is expressed in non-dimensional form by using the formula $t_N = tD_{B_1}$). It is evident from Fig. 4 that the *J*-integral value decreases with increasing of the time. This

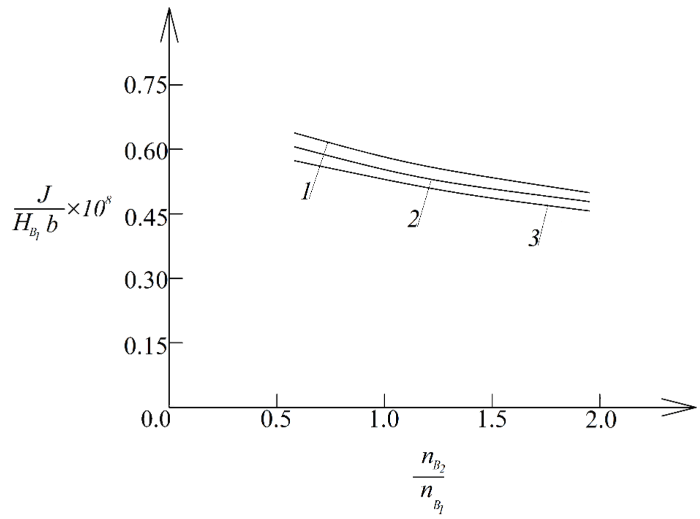


Fig. 10 The *J*-integral value in non-dimensional form presented as a function of $n_{B_2}/n_{B_1}$ ratio (curve 1-at $n_{B_3}/n_{B_1} = 0.5$, curve 2-at $n_{B_3}/n_{B_1} = 1.5$ and curve 3-at $n_{B_3}/n_{B_1} = 2.5$)

finding is attributed to the relaxation behavior. It can also be observed in Fig. 4 that the *J*-integral value is lower when the delamination crack is located between layers 1 and 2.

The influence of material parameter, $f_1$, on the *J*-integral value is evaluated (the three-layered beam configuration with a delamination crack located between layers 2 and 3 is considered (Fig. 3b)). For this purpose, the *J*-integral value in non-dimensional form is presented as a function of $f_1$ in Fig. 5 at three values of $\phi$. The curves in Fig. 5 indicate that the *J*-integral value increases with increasing of $f_1$ (this means that lower values of $H_1$ are unfavorable for delamination in sense that lower values of $H_1$ cause increase of the *J*-integral under non-linear relaxation). One can observe also in Fig. 5 that increase of $\phi$ leads to increase of the *J*-integral value.

An investigation of the effect of material parameter, $g_1$, on the *J*-integral is performed. The results of the investigation are shown in Fig. 6 where the *J*-integral value in non-dimensional form is presented as a function of $g_1$ at three thicknesses, $h_l$, of the layers. The three-layered beam with a delamination crack between layers 2 and 3 (Fig. 3(b)) is analyzed. The curves in Fig. 6 show that *J*-integral value increases with increasing of $g_1$ (this means that lower values of $D_1$ is unfavorable for delamination since lower values of $D_1$ cause increase of the *J*-integral under non-linear relaxation). Concerning the effect of the thickness of the layers, the analysis reveals that the *J*-integral value decreases with increasing of $h_l$ (Fig. 6).

The effect of material parameter, $s_1$, on the *J*-integral value is investigated too. For this purpose, calculations of the *J*-integral value are carried-out at various values of $s_1$. The three-layered beam configurations depicted in Fig. 3 are considered. One can get an idea about the effect of $s_1$ on the *J*-integral value from Fig. 7 where the *J*-integral value in non-dimensional form is presented as a function of $s_1$. The curve in Fig. 7 indicates that the *J*-integral value increases with increasing of $s_1$ (thus, decrease of $n_1$ generates increase of the *J*-integral value under non-linear relaxation, therefore decrease of $n_1$ is unfavorable for delamination). One can observe also in Fig. 7 that the *J*-integral value for the beam with delamination crack located between layers 2 and 3 is higher in comparison with that for the beam with delamination between layers 1 and 2.

The influence of $H_{B_2}/H_{B_1}$ and $H_{B_3}/H_{B_1}$ ratios on the delamination is also examined. The *J*-integral value is calculated at various $H_{B_2}/H_{B_1}$ and $H_{B_3}/H_{B_1}$ ratios for the three-layered beam structure with delamination crack located between layers 2 and 3 (Fig. 3(b)). The *J*-integral value in non-dimensional form is presented as a function of $H_{B_2}/H_{B_1}$ ratio in Fig. 8 at three $H_{B_3}/H_{B_1}$ ratios. It can be observed in Fig. 8 that the *J*-integral value decreases with increasing of $H_{B_2}/H_{B_1}$ and $H_{B_3}/H_{B_1}$ ratios (this finding indicates that the situation of increasing of $H_{B_2}/H_{B_1}$ and $H_{B_3}/H_{B_1}$ ratios is favorable for the delamination since in this situation the *J*-integral decreases).

An analysis of the variation of the *J*-integral value with increasing of $D_{B_2}/D_{B_1}$ and $D_{B_3}/D_{B_1}$ ratios is developed. The beam structure with delamination crack located between layers 2 and 3 is considered (Fig. 3(b)). The results of calculations of the *J*-integral value are illustrated in Fig. 9 where the *J*-integral in non-dimensional form is presented as function of $D_{B_2}/D_{B_1}$ ratio at three $D_{B_3}/D_{B_1}$ ratios. It can be concluded form Fig. 3 that the increase of $D_{B_2}/D_{B_1}$ and $D_{B_3}/D_{B_1}$ ratios leads to decrease of the *J*-integral value (thus, it can be concluded that the increase of $D_{B_2}/D_{B_1}$ and $D_{B_3}/D_{B_1}$ ratios is favorable for the delamination).

Finally, the effect of $n_{B_2}/n_{B_1}$ and $n_{B_3}/n_{B_1}$ ratios on the delamination is studied. Calculations of the *J*-integral are carried-out at various $n_{B_2}/n_{B_1}$ and $n_{B_3}/n_{B_1}$ ratios for the beam with delamination between layers 2 and 3 (Fig. 3(b)). The effect of $n_{B_2}/n_{B_1}$ and $n_{B_3}/n_{B_1}$ ratios is examined in Fig. 10. The curves shown in Fig. 10 indicate that the *J*-integral value decreases with increasing of $n_{B_2}/n_{B_1}$ and $n_{B_3}/n_{B_1}$ ratios, i.e., increase of $n_{B_2}/n_{B_1}$ and $n_{B_3}/n_{B_1}$ ratios is favorable for the delamination.

## 4. Conclusions

A delamination analysis of a multilayered inhomogeneous beam configuration that exhibits non-linear relaxation behavior is developed. The beam under consideration consists of adhesively bonded layers. Each layer is inhomogeneous along its thickness. The number of layers is arbitrary. The layers have individual thicknesses and material properties. The beam is loaded in bending and then held so as the angle of rotation of the ends of the beam does not change with the time. The stresses in the beam decrease with time while the strains do not change. The relaxation is treated by using a non-linear stress-strain-time relation. The material properties which are involved in this relation are distributed continuously along the thickness of each layer. The delamination is analyzed by applying the *J*-integral approach. A time-dependent solution to the *J*-integral is derived. The delamination is studied also in terms of the strain energy release rate. For this purpose, a time-dependent solution to the strain energy release rate is obtained by analyzing the balance of the energy in the beam. The strain energy release rate matches exactly the *J*-integral value (this fact proves the correctness of the solutions obtained). The variation of the *J*-integral value with time is studied. The analysis indicates that the *J*-integral value decreases with time (this behavior is due to the non-linear relaxation). Concerning the influence of the delamination crack location along the thickness of the beam, the calculations show that the *J*-integral value decreases with increasing of the thickness of the lower delamination crack arm. It is found that the *J*-integral value increases with increasing of $f_1$, $s_1$ and $g_1$. The effect of $H_{B_2}/H_{B_1}$, $H_{B_3}/H_{B_1}$, $D_{B_2}/D_{B_1}$, $D_{B_3}/D_{B_1}$, $n_{B_2}/n_{B_1}$ and $n_{B_3}/n_{B_1}$ ratios on the delamination is also investigated. For this purpose, calculations of the *J*-integral value are performed at various $H_{B_2}/H_{B_1}$, $H_{B_3}/H_{B_1}$, $D_{B_2}/D_{B_1}$, $D_{B_3}/D_{B_1}$, $n_{B_2}/n_{B_1}$ and $n_{B_3}/n_{B_1}$ ratios. It is found that the increase of these ratios leads to decrease of the *J*-integral value. The results obtained in the present paper can be used when assessing the time-dependent delamination of multilayered inhomogeneous beam structures which exhibit non-linear relaxation behavior in their life-time.

## References

Arefi, M. (2014), "Nonlinear analysis of a functionally graded beam resting on the elastic nonlinear foundation", *J. Theor. Appl. Mech*., **44**(2), 71-82. https://doi.org/10.2478/jtam-2014-0011.

Arefi, M. (2015), "Elastic solution of a curved beam made of functionally graded materials with different cross section", *Steel Compos. Struct.*, **18**(3), 2015, 659-672. https://doi.org/10.12989/scs.2015.18.3.659.

Arefi, M. and Rahimi, G.H. (2013), "Non linear analysis of a functionally graded beam with variable thickness", *Sci. Res. Essay.*, **8**(6), 256-264. https://doi.org/10.5897/SRE10.342.

Broek, D. (1986), *Elementary Engineering Fracture Mechanics*, Springer.

Butcher, R.J., Rousseau, C.E. and Tippur, H.V. (1999), "A functionally graded particulate composite: Measurements and failure analysis", *Acta. Mater.*, **47**(2), 259-268. https://doi.org/10.1016/S1359-6454(98)00305-X.

Dolgov, N.A. (2002), "Effect of the elastic modulus of a coating on the serviceability of the substrate-coating system", *Strength Mater.*, **37**(2), 422-431. https://doi.org/10.1007/s11223-005-0053-7.

Dolgov, N.A. (2005), "Determination of stresses in a two-layer coating", *Strength Mater.*, **37**(2), 422-431. https://doi.org/10.1007/s11223-005-0053-7.

Dolgov, N.A. (2016), "Analytical methods to determine the stress state in the substrate-coating system under mechanical loads", *Strength Mater.*, **48**(1), 658-667. https://doi.org/10.1007/s11223-016-9809-5.

Dowling, N.E. (2013), *Mechanical Behaviour of Materials*, Person.

Gasik, M.M. (2010), "Functionally graded materials: Bulk processing techniques", *Int. J. Mater. Prod. Technol.*, **39**(1-2), 20-29. https://doi.org/10.1504/IJMPT.2010.034257.

Han, X., Xu, Y.G. and Lam, K.Y. (2001), "Material characterization of functionally graded material by means of elastic waves and a progressive-learning neural network", *Compos. Sci. Technol.*, **61**(10), 1401-1411. https://doi.org/10.1016/S0266-3538(01)00033-1.

Hedia, H.S., Aldousari, S.M., Abdellatif, A.K. and Fouda, N.A. (2014), "New design of cemented stem using functionally graded materials *(FGM)*", *Biomed. Mater. Eng*., **24**(3), 1575-1588. https://doi.org/10.3233/BME-140962.

Hirai, T. and Chen, L. (1999), "Recent and prospective development of functionally graded materials in Japan", *Mater Sci. Forum*, **308-311**(4), 509-514. https://doi.org/10.4028/www.scientific.net/MSF.308-311.509.

Kurşun, A. and Topçu, M. (2013), "Thermal stress analysis of functionally graded disc with variable thickness due to linearly increasing temperature load", *Arab. J. Sci. Eng.*, **38**, 3531-3549. https://doi.org/10.1007/s13369-013-0626-x.

Kurşun, A., Kara, E., Çetin, E., Aksoy, Ş. and Kesimli, A. (2014), "Mechanical and thermal stresses in functionally graded cylinders", *Int. J. Mech., Aerosp., Indus., Mechatron. Manuf. Eng.*, **8**(2), 303-308. https://doi.org/10.5281/zenodo.1090725.

Kurşun, A., Topçu, M. and Yücel, U. (2012), "Stress analysis of a rotating FGM circular disc with exponentially-varying properties", *Proceedings of the ASME 2012 International Mechanical Engineering Congress & Exposition IMECE2012*, Houston, Texas, November.

Mahamood, R.M. and Akinlabi, E.T. (2017), *Functionally Graded Materials*, Springer.

Markworth, A.J., Ramesh, K.S. and Parks, Jr. W.P. (1995), "Review: Modeling studies applied to functionally graded materials", *J. Mater. Sci.*, **30**(3), 2183-2193. https://doi.org/10.1007/BF01184560.

Miyamoto, Y., Kaysser, W.A., Rabin, B.H., Kawasaki, A. and Ford, R.G. (1999), *Functionally Graded Materials: Design, Processing and Applications*, Kluwer Academic Publishers, Dordrecht/London/Boston.

Nemat-Allal, M.M., Ata, M.H., Bayoumi, M.R. and Khair-Eldeen, W. (2011), “Powder metallurgical fabrication and microstructural investigations of Aluminum/Steel functionally graded material”, *Materi. Sci. Appl.*, **2**(5), 1708-1718. https://doi.org/10.4236/msa.2011.212228.

Nguyen, S.N., Lee, J. and Cho, M. (2015), “Efficient higher-order zig-zag theory for viscoelastic laminated composite plates”, *Int. J. Solid. Struct.*, **62**, 174-185. https://doi.org/10.1016/j.ijsolstr.2015.02.027.

Nguyen, S.N., Lee, J., Han, J.W. and Cho, M. (2020), “A coupled hygrothermo-mechanical viscoelastic analysis of multilayered composite plates for long-term creep behaviors”, *Compos. Struct.*, **242**, 112030. https://doi.org/10.1016/j.compstruct.2020.112030.

Rizov, V. (2022), “Effects of periodic loading on longitudinal fracture in viscoelastic functionally graded beam structures”, *J. Appl. Comput. Mech.*, **8**, 370-378. https://doi.org/10.22055/JACM.2021.37953.3141.

Rizov, V. and Altenbach, H. (2020), “Longitudinal fracture analysis of inhomogeneous beams with continuously varying sizes of the cross-section along the beam length”, *Frattura ed Integrità Strutturale*, **53**, 38-50. https://doi.org/10.3221/IGF-ESIS.53.04.

Rizov, V. and Altenbach, H. (2022), “Multilayered frame structure subjected to non-linear creep: A delamination analysis”, *Couple. Syst. Mech.*, **11**, 217-231. https://doi.org/10.12989/csm.2022.11.3.217.

Rizov, V. and Altenbach, H. (2022a), “Multi-layered non-linear viscoelastic beams subjected to torsion at a constant speed: A delamination analysis”, *Eng. Trans.*, **70**, 53-66. https://doi.org/10.24423/EngTrans.1720.20220303.

Rizov, V.I. (2019), “Influence of sine material gradients on delamination in multilayered beams”, *Couple. Syst. Mech.*, **8**(1), 1-17. https://doi.org/10.12989/csm.2019.8.1.001.

Rizov, V.I. (2020), “Longitudinal fracture analysis of inhomogeneous beams with continuously changing radius of cross-section along the beam length”, *Strength Fract. Complex.*, **13**, 31-43. https://doi.org/10.3233/SFC-200250.

Rizov, V.I. (2020a), “Longitudinal fracture analysis of continuously inhomogeneous beam in torsion with stress relaxation”, *Struct. Integr. Procedia*, **28**, 1212-122. https://doi.org/10.1016/j.prostr.2020.11.103.

Saiyathibrahim, A., Subramaniyan, R. and Dhanapl, P. (2016), “Centrefugally cast functionally graded materials-Review”, *International Conference on Systems, Science, Control, Communications, Engineering and Technology*, 68-73.

Shrikantha Rao, S. and Gangadharan, K.V. (2014), “Functionally graded composite materials: an overview”, *Procedia Mater. Sci.*, **5**(1), 1291-1299. https://doi.org/10.1016/j.mspro.2014.07.442.

Wu, X.L., Jiang, P., Chen, L., Zhang, J.F., Yuan, F.P. and Zhu, Y.T. (2014), “Synergetic strengthening by gradient structure”, *Mater. Res. Lett.*, **2**(1), 185-191. https://doi.org/10.1080/21663831.2014.935821.


*AI*